nature methods

SUPPLEMENTARY INFORMATION

https://doi.org/10.1038/s41592-018-0015-1

In the format provided by the authors and unedited.

A comparison of methods to assess cell mechanical properties

Pei-Hsun Wu[1]*, Dikla Raz-Ben Aroush[2], Atef Asnacios[3]*, Wei-Chiang Chen[1], Maxim E. Dokukin[4], Bryant L. Doss[5], Pauline Durand-Smet[3], Andrew Ekpenyong[6], Jochen Guck[6]*, Nataliia V. Guz[7], Paul A. Janmey[2]*, Jerry S. H. Lee[1,8], Nicole M. Moore[9], Albrecht Ott[10]*, Yeh-Chuin Poh[9], Robert Ros[5]*, Mathias Sander[10], Igor Sokolov[4]*, Jack R. Staunton[5], Ning Wang[9]*, Graeme Whyte[6] and Denis Wirtz[1]*

[1]Department of Chemical and Biomolecular Engineering and Departments of Pathology and Oncology, The Johns Hopkins University and Johns Hopkins School of Medicine, Baltimore, MD, USA. [2]Institute for Medicine and Engineering, University of Pennsylvania, Philadelphia, PA, USA. [3]Laboratoire Matière et Systèmes Complexes, Unité Mixte de Recherche 7057, Centre National de la Recherche Scientifique (CNRS) and Université Paris-Diderot (Paris 7), Sorbonne Paris Cité, Paris, France. [4]Department of Mechanical Engineering, Tufts University, Medford, MA, USA. [5]Department of Physics, Arizona State University, Tempe, AZ, USA. [6]Biotechnology Center, Technische Universität Dresden, Dresden, Germany. [7]Department of Physics, Clarkson University, Potsdam, NY, USA. [8]Center for Strategic Scientific Initiatives, National Cancer Institute, Bethesda, MD, USA. [9]Department of Mechanical Science and Engineering, College of Engineering, University of Illinois at Urbana–Champaign, Urbana, IL, USA. [10]Biological Experimental Physics Department, Saarland University, Saarbruecken, Germany. *e-mail: pwu@jhu.edu; atef.asnacios@univ-paris-diderot.fr; jochen.guck@biotec.tu-dresden.de; janmey@mail.med.upenn.edu; albrecht.ott@physik.uni-saarland.de; Robert.Ros@asu.edu; Igor.Sokolov@tufts.edu; nwangrw@illinois.edu; wirtz@jhu.edu

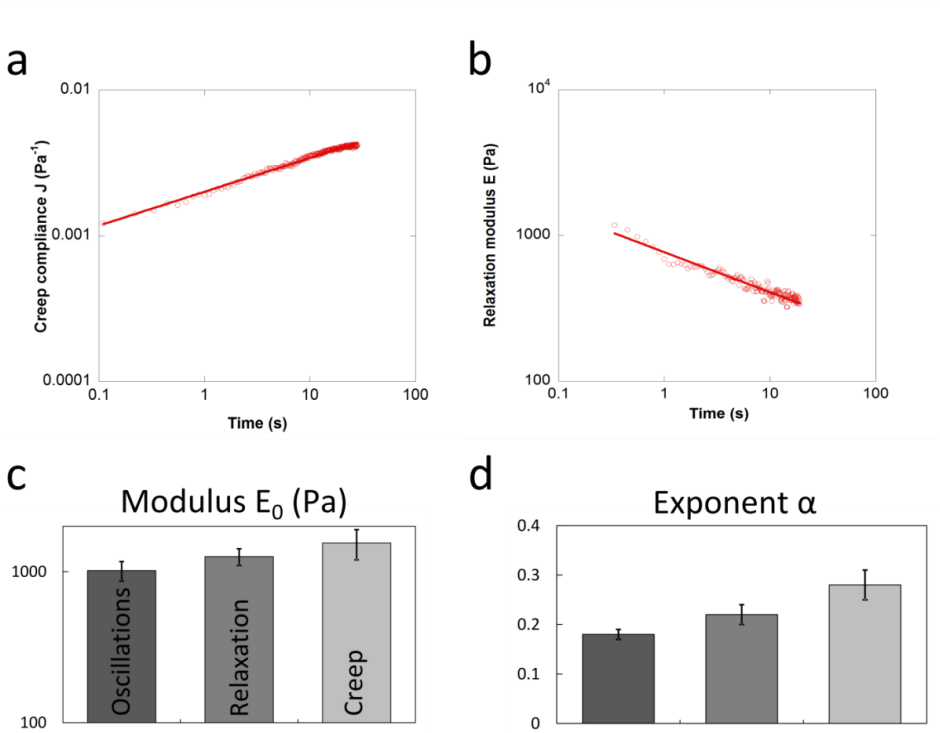

Supplementary Figure 1

Relaxation and creep functions of individual cells with the parallel-plate rheometer.

a, Typical creep function obtain for MCF 7 cell. b, Typical relaxation function obtain for MCF 7 cell. c, diagram representing the mean of the extensional modulus at 1Hz obtain for the different tests performed on MCF 7 cells with the parallel plates technique. (n=18 for the oscillation test, n=15 for the relaxation test, n =11 for the creep test). d, mean of the exponent of the power law found for the corresponding rheological tests in c. Error bars are standard errors..

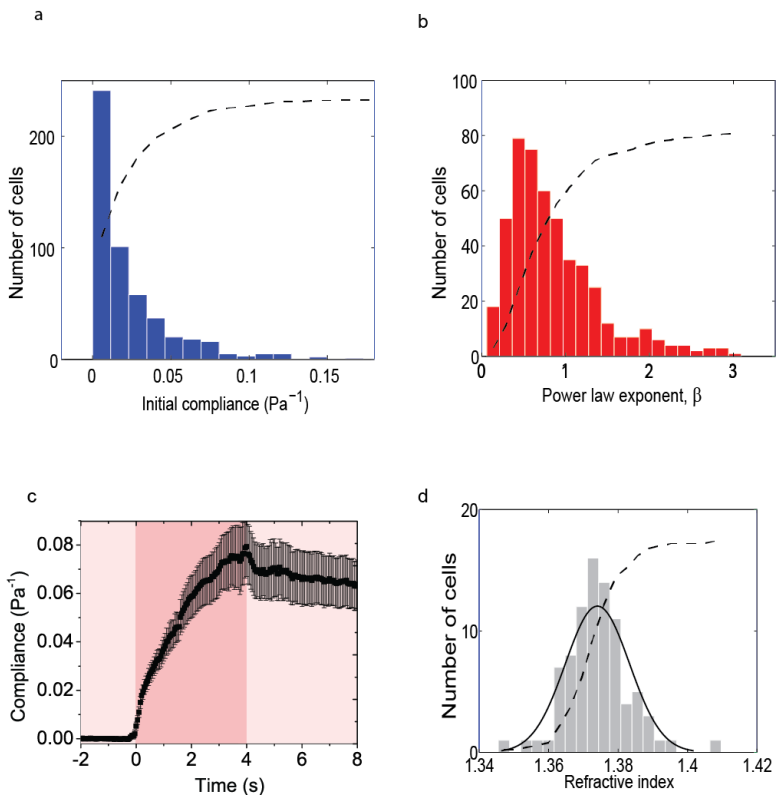

Supplementary Figure 2

Further analysis and details of OS results.

a Distribution of initial compliance J_o for each MCF7 cell stretched (n = 514), based on the power law model. The dotted line represents the cumulative distribution. **b** Distribution of the power law exponent β. The average β here was found to be 0.85 ± 0.03. **c**. Average compliance curve for 11 MCF7 cells stretched using 1.5 W per fibre, showing more typical viscoelastic features than the cells stretched at 0.7 W per fibre as in the main text. **d** Distribution of the average refractive index obtained for 89 cells. Here, the population average is 1.374 ± 0.002.

Supplementary Information

Supplementary note 1

Glossary

See also Fig. 1.

Stress – force per unit area; $\sigma = F / A$ SI unit is N/m^2

Strain –unitless parameter quantifying the extent of deformation after application of mechanical stress.

Compliance **(*J*)** – the relative extent to which a body yields to deflection by force, usually given by time dependent strain divided by constant stress

Shear Stress **(σ)** – force parallel to a material's axis per unit area; $\sigma = F / A$

Shear Strain **(γ)** –unitless parameter quantifying the extent of deformation after application of shear stress. For a cube, shear strain is ratio of lateral displacement over sample height. For other shapes, the form factor relates measured displacement to unitless strain.

Elongational Strain **(ε)** – fractional change in length or elongation; $\varepsilon = \delta / L$

Elasticity – the property of a material to deform to a defined extent in response to a force and then return to its original state when the force is removed

Viscosity **(η)** – measure of resistance of a fluid to deformation in response to shear stress; $\eta = \sigma / d\gamma/dt$

Young's modulus **(E)** – a constant describing a material's resistance to deformation in extension; $E = \sigma / \varepsilon$

Shear Modulus **(G)** – a constant describing a material's resistance to deformation in shear; $G = \sigma / \gamma$

Linear elasticity – Young's or shear modulus constant over range of strains, equivalently stress is proportional to strain.

Newtonian viscosity – viscosity independent of shear strain rate; linear relationship between shear stress and shear strain rate

Nonlinear elasticity – Young's or shear modulus that changes with strain

Non-Newtonian viscosity – viscosity dependent on shear strain rate; non-linear relationship between stress and strain rate (i.e. shear thickening or thinning)

Yield stress **(σ_y)** – maximum stress applicable to a system before

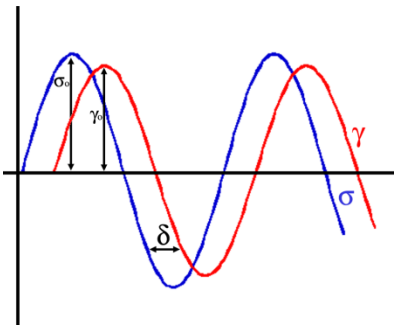

Stress σ_0 and strain γ_0 amplitudes against time in an oscillatory deformation. The stress and strain signals are phase shifted by an angle δ.

rupture occurs

Poisson ratio (v) – the ratio of transverse to axial strain when a material is deformed in stretch or compression. A material that conserves volume under strain has a Poisson ratio of 0.5. Materials with Poisson ratio less than 0.5 lose volume when compressed and gain volume when stretched. For linear elastic materials at small strain, Poisson's ratio relates shear and Young's moduli by the expression $E = 2G(1+\nu)$.

Dynamic viscoelasticity – Many time-dependent rheological measurements are made by applying a sinusoidally varying stress or a sinusoidally varying strain to a sample and measuring its strain or stress response, respectively, as a function of frequency. For linear materials, the result is two sinusoidal functions, and both the elastic and dissipative properties of the material are computed from the amplitudes and phase shifts of the sinusoidal functions.

Phase angle (δ) – The angular shift between the sinusoidally varying stress and strain in an oscillatory measurement. The value of δ is zero for a purely elastic solid and 90 degrees for a purely viscous liquid.

Elastic or storage modulus **(*G'*)** – measure of energy stored during a strain cycle; under sinusoidal conditions, the part of shear stress in phase with shear strain divided by shear strain; often expressed as the real part of the complex modulus: $G' = (\sigma_o / \gamma_o)*\cos(\delta)$

Viscous of loss modulus **(*G"*)** – measure of energy lost during a strain cycle; often expressed as the imaginary part of the complex modulus: $G'' = (\sigma_o / \gamma_o)*\sin(\delta)$

Supplementary note 2

Introduction to viscoelastic materials

Viscoelastic moduli are commonly used to describe both static and dynamic measurements of mechanical properties of materials. The methods considered in this paper allow us to measure either static or dynamic moduli, or both. Three primary moduli of elasticity are typically used by experts: the Young's modulus (compression/extension), the shear modulus, and the bulk modulus. The Young's modulus (usually denoted E) is generally measured by applying a uniaxial stress perpendicular to one of the surfaces of the sample to deform it either in compression or extension. The modulus is then measured as a function of the force per unit area (stress) and as a function of the relative change in length of the sample (strain). An important feature of Young's moduli measurements, especially for hydrated samples, is that the volume of the sample is not necessarily conserved during such deformations. The extent to which a sample changes its volume, or equivalently the relationship between changes in vertical dimension and in the two

orthogonal dimensions, is quantified by the Poisson's ratio. If the sample maintains a constant volume, the Poisson's ratio is 0.5. If the sample loses volume in compression or gains volume in extension, then the Poisson's ratio is < 0.5. The shear modulus (usually denoted *G*) is measured by applying a force parallel to the surface of the sample. An important feature of shear deformations is that they maintain the volume during application of the force, regardless of what the Poisson's ratio is. Finally, the bulk modulus (usually denoted *K*) is measured by applying forces on all surfaces of the sample and determining the volume change as a function of applied force per unit area, it corresponds to the inverse of the compressibility. For biological samples that are mostly water, true bulk moduli are almost never measured since water is nearly incompressible.

General principal of viscoelasticity test

For a surface of area *A*, the applied (normal) stress is given by $\sigma = F/A$, and the deformation (or strain) in the direction of the applied force is $\varepsilon = \Delta L/L_o$, and $\Delta L = L\text{-}L_0$ is the sample elongation along the direction of stretching. The mechanical response of any material can be described as a combination of two ideal behaviors, those of an elastic solid and of a viscous liquid. Purely elastic solids, like springs, deform instantaneously and in proportion to the applied force. In creep, the strain sets instantaneously to its equilibrium value ε_i. In dynamic tests, the deformation follows the oscillating applied stress, meaning that there is no phase shift between $\varepsilon(t)$ and $\sigma(t)$ signals. In both tests, the ratio between stress and strain is constant and corresponds to the elastic modulus $E = \sigma/\varepsilon$, which is expressed in Pascals (Pa). The modulus *E* quantifies the rigidity of the material. Like springs, solids with high *E* are harder to deform. Purely viscous fluids, like water, will flow indefinitely when subjected to a creep test. The rate $d\varepsilon/dt$ at which the liquid flows under a given stress σ_0 depends on its viscosity η, $\delta\varepsilon/\delta\tau = \sigma_0/\eta$. In dynamic tests, the oscillating deformation is delayed compared to the applied oscillating stress, and the phase shift between $\varepsilon(t)$ and $\sigma(t)$ signals is $\Delta t = T/4$, where *T* is the period of the oscillations. The amplitudes of stress and strain are then related by $\sigma = (2\pi f\eta)\varepsilon$, where $f = 1/T$ is the frequency of the oscillations. Thus $(2\pi f\eta)$ has the dimension of a modulus, and quantifies the viscous response depending on the frequency of the test.

Most materials are viscoelastic and share characteristics of both elastic solids and viscous liquids. Depending on the time scale (or, equivalently, on the frequency), the elastic or viscous-like behavior may dominate the response of such material. In dynamic tests, the phase shift between $\varepsilon(t)$ and $\sigma(t)$ will be between 0 and $T/4$. The response of the viscoelastic sample is then quantified through a complex modulus $E^* = E' + i\,E''$, allowing one to decouple the elastic-like contribution E' (the in-phase component of the response) from the viscous-like component E'' (phase shift $\Delta t = T/4$). In the particular example of the figure, $E' = E$ the elastic modulus of springs, and $E''= 2\pi f\eta$, where η is the viscosity of the surrounding liquid and f the frequency of the oscillations. Thus, at high frequency (short times) $E'' > E'$ and the viscous behavior dominates, while at low frequency (long times) $E' > E''$ and the behavior is dominantly elastic, as observed from a creep test.

Supplementary note 3

Comparison between different methods

In principle, different types of rheological measurements should be related to each other if certain assumptions about the materials being measured are valid. It is likely that some discrepancies in the literature arise from assuming that cells and other biological materials are linear elastic continuous solids. Cells, however, are far from being isotropic, and real measurements require finite, sometimes large strains to obtain reliable force data. Nearly all measurements by surface indentation, for instance, assume the validity of the equation relating E and G because the deformation in such measurements is a complex combination of uniaxial and shear deformations that change with indentation depth and probe geometry. Recent measurements on macroscopic biological samples suggest that Young's and shear moduli are not simply related under the conditions of many studies. For example, Young's and shear moduli during macroscopic measurements of biopolymer networks such as collagen networks (1; 2) and intact biological tissues (3; 4) become uncoupled from each other at deformations as small as a few percent. Since the typical deformations applied by AFM probes and possibly also magnetic tweezers are far larger than this value, these measurements are likely to depend on the extent to which uniaxial and shear deformations dominate the deformation, a quantity that is usually unknown.

The measurements using the large AFM probes are physically quite similar to the whole-cell measurements using parallel-plates rheometry. The values of the elastic modulus derived by both methods are indeed not substantially different (see Table 1). Smaller values derived from the AFM measurements can be explained by examining the difference in the physics of the probe-cell contact in these two methods. While forces are applied to the cell directly due to physical contact in AFM, the parallel plates apply forces through molecular links developed between the plates and the cell body. Physical indentation of the cell with the AFM probe implies squeezing of both the pericellular coat and the cell body itself. Since the pericellular coat is effectively softer than the cell body (5; 6), the AFM values of the elastic modulus are expected to be smaller than the values obtained by parallel-plates rheometry. Using a more complicated model, which takes into account the presence of the pericellular layer (7), it is possible to derive the elastic modulus of the cell body in the AFM experiments. As one can see from ref (8), the values obtained within such a model for MFC-7 cells (0.95±0.26 kPa) are virtually identical to the values obtained with the parallel-plates rheometer (0.95 ± 0.15 kPa, see Table 1).

AFM can also be directly compared with MTC. Similar to the parallel-plates approach, the contact between the magnetic bead and cell is due to molecular linkages between the bead and pericellular membrane. However, the modulus derived from MTC data is about ~60% higher than even the one derived from parallel-plates rheometer. This could be explained by the fact that the effective area of the contact between the magnetic bead and cell is higher than assumed due to additional contact between the beads and microscopic roughness of the pericellular membrane (microvilli and microridges).

The second assumption underlying most mechanical measurements of cells is that the Poisson's ratio is close to 0.5, or at least is a constant. However as is well-documented in the literature for tissues such as cartilage, many biological materials are highly poroelastic, with stresses relaxing as fluid flows out of a compressed network or into a stretched network, allowing the polymers to adopt lower energy states. In macroscopic rheological measurements of elasticity, poroelasticity is often negligible because the fluid permeation is so slow that the volume cannot change during the measurements on a time scale of a second or so. However, measurements of cells by nanoscale indenters deform very small volumes of material, and since the poroelastic relaxation time is a function of sample size, the rate in which fluid flows out of the deformed volume can be significant. In this case the assumption that the Poisson's ratio is a

constant during the measurement is invalid and is likely to affect measurements that occur on different length scales or timescales.

Primary *vs*. model-based data

In an attempt to further compare our various measurement methods, physical models are used, and with these, certain assumptions are introduced, such as linear elasticity for AFM or viscoelastic behavior for the other methods. In this context, a distinction should be made between primary and unprocessed data, and the inference from these measurements on the parameters commonly used to describe the material properties of the cell.

Using MTC as an example, primary data include the known torque applied to each bead, and its resulting displacement. For this case, one typically assumes values for the surface area of the bead in direct contact with the cell (or the contact area can be measured by staining the ligand or the receptor or the nearby recruited proteins), that the cell can be treated as a homogeneous, isotropic, linear, viscoelastic material [15], and that the stresses generated by the twisting torque is directly transmitted to the cell regardless of the receptor/ligand interactions used to attach the bead. Most of the same assumptions apply to the interpretation of data from AFM measurements, where the primary data are generally uniaxial force and displacement, and calculations of material constants account for the complex strain field due to the tip geometry.

A number of analytical and approximate models are used for pyramidal, conical, spherical, blunted, and spheroconical tips, wherein the power law exponent varies from ½ (conical) to 3/2 (spherical). Discrepancies arising from the choice of model typically range within other sources of systematic error (e.g. cantilever calibration errors ~10-15%) and from the assumption that shear and Young's moduli are simply related (see glossary), since AFM probes typically result in spatially complex strains fields that combine shear, compression, and stretch (2; 3). These models yield an elastic modulus, which assume a homogeneous, isotropic, and linear elastic material. In the quasistatic deformations used here (indentation rates ~1 – 10 μm/s), cells characteristically exhibit an elastic response for which the timescale for which dissipation is minute. Dynamic mechanical analysis whereby the AFM tip is oscillated over a range of frequencies while in contact with cell can also be conducted, yielding a complex (i.e. viscous and elastic) modulus (9; 10). In cases where specific adhesion is strong, contact area is increased, changing the strain field, for which other models may be used (11). If these assumptions are

valid, the computed elastic modulus values are precise and accurate; but for cells, these assumptions are at best only partially satisfied – e.g., the cell cortex, cytoplasm and nucleus each have uniquely different characteristics. Consequently, errors may be introduced in transforming the primary data into the material properties. Similar assumptions are made in the calculation of moduli from other experimental methods. Further, recent work indicates that the cytoplasm of living cells can behave as a poroelastic material, which could potentially result in errors in estimating moduli from primary data (12).

Effects of mechanical stress and frequency

The response of a living cell to a mechanical stimulus depends on how it is applied. Oscillating CMR yields a notable decrease of the cell modulus with increasing amplitude regardless whether it is deformation (also called strain) or stress that is controlled. Moduli measured by AFM show a rather large difference when measured with sharp or dull AFM probes (Fig.2). These can be explained by substantial difference in the stresses imposed by such probes onto the cell. In addition, AFM allows measuring the moduli's dependence on the indentation depth though there is no clear overall trend, and both increasing and decreasing moduli occur. Cells are known to exhibit stiffening as well as softening and the complex interplay between the two is still far from understood.

Besides the size of the probe, cells are also sensitive to the probed timescales. Passive and active microbead rheology show that cell moduli increase with frequency. This is in good agreement with the parallel-plates rheometer as well as CMR results. They yield moduli that increase with frequency as a weak power-law with an exponent in the range of 0.01-0.25. Cell deformability (also called compliance) obtained from creep experiments also increases as a weak power law with time. The exponents are similar to those obtained from frequency sweeps as measured by the parallel-plates rheometer and CMR. The CMR study shows that the exponent depends on the applied stress (see supplementary information). The OS also yields a power-law increase for cell compliance. However, the exponent is 0.85, close to one, indicating a mostly viscous behavior of the cells. This is presumably because the OS probes cells in suspension, for which the main force-bearing structures of the attached cell – stress fibers and focal adhesions – are absent.

A deformation of controlled amplitude and frequency defines a rate. We observe that the cell response is highly dependent on the rate of deformation. For AFM measurements, indentation speeds can be varied between 2 and 10 μm/s. However, no clear dependence of the moduli on the rate can be inferred. This may be attributed to the fact that the modulus was measured at a relatively large indentation of 1μm. This means that the pericellular layer of cell was squeezed and, consequently, we probed the mechanics of the cell body. As was recently found for neuronal cells(5), the mechanics of the cell body is independent of the indentation speed for indentation rates of 1–10 μm/s, which is similar to the range used in this paper. Cell monolayer rheology probes cell responses to shear stress ramp cycles of different speeds. A pronounced hysteresis between loading and unloading occurs for slow rates of stress increase or decrease. The amplitude of the hysteresis corresponds to the amount of energy that is absorbed by the cell in a loading and unloading cycle. Hysteresis vanishes above a threshold rate and the cell deformation is almost dissipation-free. We suggest that above a certain stress rate cytoskeletal bonds do not reform (13), and the cell exhibits a mostly elastic response. Cellular moduli may vary by up to an order of magnitude depending on size, frequency, and rate of the mechanical cues, which can be probed with the different experimental approaches described in this work.

Adherent *vs.* free-floating cells

The elasticity of MCF-7 cells measured by OS was more than two orders of magnitude smaller than the elasticity measured by AFM, MTC, and parallel-plates rheometer. The major difference between OS and the other techniques is in the cell adhesion: OS deals with free-floating cells, whereas the other methods use cells adhered to a rigid glass substrate. Although it is expected that cells change their cytoskeleton, and presumably their mechanical properties, after adhesion, it was shown that weakly adherent MCF-7 cells do not significantly change their modulus (6). This implies that complete detachment of cells from the surface substantially “relaxes” cells. It should be noted that the OS is the ideal technique to assess the mechanical properties of naturally suspended cells, such as blood cells or circulating tumor cells. The cells being in suspension also enables higher measurement throughput (> 100 cells/h) compared to techniques where cells are attached to a substratum.

Dependency of mechano-transduction signaling

MTC and the CMR employ an "active" mechanical measurement where specific ligands are used. MTC utilizes beads that are coated with RGD peptides, while CMR has fibronectin-coated plates to engage specific transmembrane integrins in cell adhesion. In such conditions, the cellular cytoskeleton is connected to integrins cell-receptors through focal adhesion complexes, and tensile forces are generated in the cell structure and transmitted to its substrate (in particular to the mechanical probe). Mechanical measurements can then propagate deeply into the cell through prestress and stiff actin bundles that guide the propagation of forces over long distances (14). Parallel-plates rheometry, PTM, AFM, and OS probe relaxed cells since no extracellular matrix proteins are engaged. However, although not done in this study, parallel-plates rheometry and AFM are capable of active mechanical measurements on mechanically active (i.e. tensed) cells by functionalizing the surfaces with specific ligands, and high tensile forces were indeed measured in these conditions (15-17). In CMR, the measured elastic modulus is about an order of magnitude higher than the ones obtained from other contact probe based methods. This can presumably be explained by the existence of a tensile pre-stress in CMR. Indeed, since the plates of the rheometer are coated with fibronectin and cells left to spread before measurement, cells are probably applying high tensile forces in between the plates (15-17). Such a pre-stress is known to increase the apparent elastic modulus of cells, the modulus increasing roughly linearly with the pre-stress (18). In this context, one order of magnitude increase in the apparent elastic modulus, as measured with MCR, is consistent with the typical tensile stresses measured on single cells. It is also consistent with the observations of substantially higher modulus in AFM experiments when using the sharp conical AFM probe. Such probe produces much higher stresses compared to the use of the dull probes. As a result, the cell material presumably becomes overstretched and becomes stiffer. This is similar to what was observed on other soft materials and viscoelastic polymer solutions (19).

Dependence of cell mechanics and cellular processes on time scales

The cytoskeleton is a dynamic biopolymer network whose material properties are different when probed at short and long timescales (20; 21). There is emerging evidence that such timescale dependence of cytoskeletal or cellular mechanical properties correlate with different cellular functions (22). In addition to the frequencies of measurement, the overall duration that each cell

is subjected to probing has to be taken into consideration to account for time-scale dependent cellular processes. Each cell in the AFM can be measured starting from several seconds up to several hours (to obtain sufficient statistics, several minutes per cell should be expected to spend). Parallel-plates measurements were done in ~30 s per cell. For PTM, the measurements on each cell lasted about 20 s. In MTC, each cell experienced probing for 17 s. For the OS, creep stretching was conducted for 4 s and 8 s per cell. Each cell in CMR was probed for about 1.5 to 2 hours. If these measurements with the various techniques lasted longer or shorter on each cell, the results would be expected to be different owing to changes taking place in each cell during the time of probing. We consider such timescale dependent cellular processes.

Signaling, transcription processes and protein synthesis (which alter cell state and architecture) can take different amount of time to process (minutes for phosphorylation and hours for transcription) . Actin polymerization and cytoskeletal remodeling also take place in seconds (23). Changes in cell mechanics and cell shape to effect protrusion and migration takes place in minutes (24). Taking a closer look at the timescales involved in various cellular processes, one would find it justifiable to think of 'time factor' in cell functions involving mechanical properties. Adherent cells in 3D may be predominantly elastic over short timescales (< s) in order to withstand sudden forces from surrounding cells, while over longer timescales they become more fluid like or viscous, to migrate better, thereby impinging on metastasis in the case of cancer cells.

The 'time factor' may well turn out to be one of the sources of some of the similarities and differences in the results. It becomes necessary to care about the duration of mechanical perturbation to which each the cell is subjected during measurement, in view of the time evolution of the property involved (25), as a clear example of time-dependent changes in cell deformability. At the same time, the change of mechanical properties is not necessarily large. AFM measurements of human epithelial skin cells showed virtually the same modulus during continuous measurements for about 2.5 h (26).

Limitation of the results

Though the goal of this work is to directly compare different cell mechanical methods by probing the same type of cells with minimal biological variations, systematic errors may arise from the different instrumentations setups, which could also contribute to the observed wide

spectrum of results. For example, distinct from other methods presented here, sample heating is one of primary source of systematic error for OS. Cells measured with OS at different temperatures (e.g. induced by the stretching laser) leads to a shortening of the time-scales at which the cells respond. The impact for the measurement here is that the OS as used in the present study (laser wavelength 1064 nm) likely led to heating, which has in turn led to a more viscous response of the cells. It should be noted that this is not due to biological change (via transcription or signaling, for example as a heat-shock response of cells), but a purely material response during the short duration of the measurement. The temperature is back to ambient temperature as soon as the laser is turned off (27). The potential source of systematic error has beene discussed in the literature, for PTM in (28; 29), for AFM in (19), for MTC in (30; 31), and for parallel plates in (32). Importantly, the reported systematic relative error is in general < 20%, while the observed difference in measured elastic moduli from these different methods can be as high as 3,000 fold.

Furthermore, in the present study, we found that AFM and PTM contribute to the highest and lowest elastic moduli measured among the six tested methods. The results were in the same range as shown in a previous study in which mechanical properties of non-tumorigenic breast epithelial MCF-10A and tumorigenic breast cancer cell MDA-MB-231 were assessed by AFM and PTM (33). The Youngs' modulus of MDA-MB-231 and MCF10A cells measured by AFM was ~ 0.2-1.6 kpa, depending on the cell type and probe location. Resulting MSD profiles from PTM were also in the similar scale as the one measured in the current comparative study. Therefore, the measurement spread between different cell mechanical assays is less likely to be due to method-dependent systematic errors, and more likely to be due to the level of mechanical **stress** and rate of deformation to which the cell is subjected, the geometry of the mechanical probe used in the experiments, the probe-cell contact area, the probed location in the cell (e.g. cell cortex, nucleus, cytoplasm), and the cellular context (e.g. monolayer of cells *vs*. single cells, adherent *vs*. free-floating cells, etc.).

Choice of methods for different biological contexts

The proper choice of a cell-mechanics method depends critically on the biological context and the biological process of interest (Table S1). All tested methods can probe cell samples *in vitro* and *ex vivo*. However, only MTC and PTM can be directly extended to probing mechanics of

cells in tissues *in vivo* or fully embedded in 3D extracellular matrices since, for both methods, the probes (i.e. the probe particles) are remotely monitored through optics and no direct contact is required from cell mechanics.

Unlike other methods, OS measures cells in suspension, without physical contact with a probe, but OS cannot probe the micromechanics of cells adherent on 2D substrates or embedded in 3D tissues and matrices. OS is an ideal choice for measuring blood-borne cells at single-cell resolution. All six methods can provide single-cell resolution, but measurement throughput can vary from <10 (parallel plates, AFM) to ~2,000 (MTC) cells per hour (Table S1). For cell samples with known large variations, higher throughput measurements, such as MTC and OS (~100 cells per hour), may overcome sample variations by collecting large datasets.

One other important factor to consider is the mechanical context associated with the biological question being asked. If the differences being investigated are local or are rapid changes in the cytosol, using PTM may provide the more sensitive readout. To probe changes in cortical tension (for instance following cell spreading), MTC is particularly well suited (Table S1).

References

1. Vahabi M, Sharma A, Licup AJ, van Oosten AS, Galie PA, et al. 2016. *Soft matter* 12:5050-60
2. van Oosten AS, Vahabi M, Licup AJ, Sharma A, Galie PA, et al. 2016. *Sci Rep-Uk* 6:19270
3. Perepelyuk M, Chin L, Cao X, van Oosten A, Shenoy VB, et al. 2016. *PloS one* 11:e0146588
4. Pogoda K, Chin L, Georges PC, Byfield FJ, Bucki R, et al. 2014. *New J Phys* 16:075002
5. Simon M, Dokukin M, Kalaparthi V, Spedden E, Sokolov I, Staii C. 2016. *Langmuir* 32:1111-9
6. Guz N, Dokukin M, Kalaparthi V, Sokolov I. 2014. *Biophys J* 107:564-75
7. Sokolov I, Dokukin ME, Guz NV. 2013. *Methods* 60:202-13
8. Dokukin ME, Guz NV, Sokolov I. 2013. *Biophys J* 104:2123-31
9. Mahaffy RE, Shih CK, MacKintosh FC, Kas J. 2000. *Physical review letters* 85:880-3
10. Alcaraz J, Buscemi L, Grabulosa M, Trepat X, Fabry B, et al. 2003. *Biophysical Journal* 84:2071-9
11. Johnson KL, Kendall K, Roberts AD. 1971. *Proc R Soc Lon Ser-A* 324:301-&
12. Moeendarbary E, Valon L, Fritzsche M, Harris AR, Moulding DA, et al. 2013. *Nat Mater* 12:253-61
13. Xu JY, Tseng Y, Wirtz D. 2000. *J Biol Chem* 275:35886-92
14. Poh YC, Chen J, Hong Y, Yi H, Zhang S, et al. 2014. *Nature communications* 5:4000
15. Mitrossilis D, Fouchard J, Guiroy A, Desprat N, Rodriguez N, et al. 2009. *Proceedings of the National Academy of Sciences of the United States of America* 106:18243-8
16. Mitrossilis D, Fouchard J, Pereira D, Postic F, Richert A, et al. 2010. *Proceedings of the National Academy of Sciences of the United States of America* 107:16518-23

17. Thoumine O, Ott A. 1997. *Journal of cell science* 110 (Pt 17):2109-16
18. Kollmannsberger P, Fabry B. 2007. *The Review of scientific instruments* 78:114301
19. Dokukin ME, Sokolov I. 2012. *Macromolecules* 45:4277-88
20. Deng L, Trepat X, Butler JP, Millet E, Morgan KG, et al. 2006. *Nature materials* 5:636-40
21. Xu J, Tseng Y, Wirtz D. 2000. *J Biol Chem* 275:35886-92
22. Ekpenyong AE, Whyte G, Chalut K, Pagliara S, Lautenschlager F, et al. 2012. *PloS one* 7:e45237
23. Yap B, Kamm RD. 2005. *Journal of applied physiology* 99:2323-30
24. Stroka KM, Hayenga HN, Aranda-Espinoza H. 2013. *PloS one* 8:e61377
25. Frank RS. 1990. *Blood* 76:2606-12
26. Berdyyeva TK, Woodworth CD, Sokolov I. 2005. *Physics in medicine and biology* 50:81-92
27. Ebert S, Travis K, Lincoln B, Guck J. 2007. *Opt Express* 15:15493-9
28. Savin T, Doyle PS. 2005. *Biophysical Journal* 88:623-38
29. Wu PH, Arce SH, Burney PR, Tseng Y. 2009. *Biophysical Journal* 96:5103-11
30. Gosse C, Croquette V. 2002. *Biophysical Journal* 82:3314-29
31. Wong WP, Halvorsen K. 2006. *Opt Express* 14:12517-31
32. Desprat N, Richert A, Simeon J, Asnacios A. 2005. *Biophysical Journal* 88:2224-33
33. Agus DB, Alexander JF, Arap W, Ashili S, Aslan JE, et al. 2013. *Scientific Reports* 3

Supplemenatry Table 1. Overview of measurement techniques

Technique	Cellular/ECM Components	Measurement Throughput	Experimental Conditions										Measured moduli	model assumtpion	directed measurement	Characteristic time	Disease Applications to Date	Advantages	Participatning Laboratories
			In vitro	In Vivo	Ex Vivo	2D	3D	Tissue	Single Cell	Adherent	Suspension	Perturbations in Real Time							
Parallel Plates	Global cell mechanics; Cell cortex; ECM	6 cells/hr	X		X	X	X	X	X	X		X	E	viscoelastic	instantaneous deflection of the flexible plate and the rigid plate displacement	0.1-100 s (0.01-10 Hz)	gastrointestinal cancer; malaria	Single-cell scale or tissue aggregates; Uniaxial geometry; Versatile setup: time or frequency-dependent measurements, analysis of passive (rheological) or active (force generation)	Asnacios lab
Optical Stretching	Global cell mechanics; Cell Cortex and cytoplasm; Nucleus [Chalut, Biophys. J. 2012]; ECM	60 - 300 cells/hr	X		X		X		X		X	X	E	viscoelastic	time-dependent compliance.	8 sec at 0.75W per fiber	breast cancer; oral squamous cancer; leukemia; Malaria	Non-invasive: No mechanical contact of measuring probe with cells during measurement; Cells in suspension; Probe multiple directions	Guck Lab
Cell Monolayer Rheology	Global cell mechanics, Adhesion strength, ECM	10^6 cells per experiment, 5-6 hr/experiment	X		X	X	X	X	X	X		X	G	viscoelastic	stress or strain	Frequency sweep: 0.1-10s (0.1-10Hz)	Heart disease	Direct assessment of a mean value of 10^6 cells in a single measurement or tissues; High reproducibility; Amplitude, frequency, force and time controlled measurements are possible; Measurement of cell adherence force is easily possible; Tissues or dense cell monolayers can be probed as well	Ott lab
Atomic Force Microscopy	Global cell modulus (spherical probe); Specific areas of cell cortex associated with lamellipodia, cytoplasm, protrusions, area over nucleus (tip probe); Glycocalyx (shallow indentation); Cell cytoplasm and nucleus (deep indentation), ECM	1- 20 cells/hr	X		X	X	X	X	X	X		X	E	linear elasticity	force-indentation curves	loading rate: 2-10μm/sec	Aging; leukemia; breast cancer; cervical cancer; Barrett's esophagus	Provide information about differences between different regions of the cell body and the depth dependence of the mechanical properties	Ros Lab Sokolov lab Janmey lab
Magnetic Twisting Cytometry	Cell cortex; Cell cytoplasm; Nucleus; ECM	2000 cells/hr	X	X	X	X	X	X	X	X		X	G	viscoelastic	magnetic bead displacement	3.3s (0.3 Hz)	Cancer; Lung disease	Investigate the effects of force applied through different specific transmembrane receptors; Allows one to apply a local force on the cell and monitor the deformations at different regions of the cell; Versatile control of the frequency and magnitude of force applied; Probe along multiple axes	Wang Lab
Ballistic Injection Nanorheology	Global cell mechanics; Cell Cytoplasm; Nucleus; ECM	30 cells/hr	X	X	X	X	X	X	X	X		X	G	viscoelastic	Mean-squared displacement of tracked nano-particles	0.03-10s (30 - 0.1 Hz)	Laminopathies; Muscular distrophy; Aging; Cancer	Single-cell resolution; Allows one to monitor the deformations at different regions of the cell; Can real-time pair with other micscopic cellular imaging method.	Wirtz lab

Supplementary Table 2. Summary of AFM measurements

Lab	Ros		Sokolov		Janmey	
AFM type	MFP-3D Bio (Asylum Research, Santa Barbara, CA) mounted on an IX-71 microscope (Olympus)		BioScope Catalyst (Veeco, Woodbury, NY)		DAFM-2X Bioscope (Veeco, Woodbury, NY) mounted on an Axiovert 100 microscope (Zeiss, Thornwood, NY)	
Z-range of scanner	~5 µm used (~25µm full)	~10 µm used (~25µm full)	10.0 µm used (~24 µm full)		~3 µm used (ramp)	
Cantilever stiffness (N/m)	0.184N/m, (Thermal tune method)	0.214N/m, (Thermal tune method)	0.0596 N/m (Thermal tune method before gluing the spherical probe)		0.06 N/m (Thermal tune method)	
Shape of probe (nm/angle)	Pyramidical, conical half-angle ~15.12° (manufacturer specs)	Conical with spherical end, R~680 nm and half-angle 22.5° (SEM images from manufacturer)	Spherical probe R~2475 nm (Inverse grid imaging)		conical tip half-angle ~15^{o} (manufacturer specs)	Spherical probe R~2500 nm (manufacturer specs)
Depth of measurement (nm)	Approx. 1000 nm average	Approx. 6000 nm average	410 - 3070 nm (Average 1300 nm)	50-3000 nm	Up to 1000nm	
Indentation rate (µm/s)	2 µm/s		10 µm/sec (~0.5Hz ramping)		6 µm/s (~1 Hz ramping)	
Length of time from first plating cell to measurement	~24 h		from plating on glass to measurement 16-18 h		36-48 h after plating the cells	
Length of time from taking cell out of incubator to measurement	~10-15 min, measurements lasted ~3 h/dish		~10-15 min, measurements lasted ~3 h/dish		~10-15 min, measurements lasted ~3 h/dish	
Temperature of measurement	37° C		37° C		Room temperature	
Data fitting method	Sneddon Model	Briscoe Model (blunted cone)	"Brush" model	Hertz model	Hertz model Linearized model	Hertz model

Mean effective Young's modulus (kPa)	Nuc.: 5.50 kPa mean; 2.91 kPa median; 0.89 kPa “mode”. Cyt.: 3.8 kPa mean; 2.5 kPa median; 1.1kPa ”mode”.	0.60 kPa mean; 0.50 kPa median; 0.35 kPa “mode”.	1.39 kPa mean; 0.98 kPa mode.	< 300 nm: 0.53 kPa mean; 0.81 kPa mode. > 300 nm: 0.74 kPa mean; 0.23 kPa mode.	300 nm: 9±3.5 kPa 700 nm: 9.5±4 kPa Linearized model: 300 nm: 6.5±3.5 kPa, 700 nm: 7.3±3 kPa	300 nm: 1.3±0.5 kPa, 700 nm: 1.3±0.6 kPa.
Variance in Young's modulus with indentation depth	Nuc: drops ~5-fold in first µm. Cyt: drops 50% in first µm	Very little change in first µm, gradual increase (~30%) over several µm	for plateau ~20 %	>160%	No significant difference in the Hertz model	
Number of cells measured	30 cells	60 cells	20 cells	20 cells	~20 cells	~10 Cells
Number of indentations per cell	10 on nucleus, 10 on cytoplasm (4 of each used)	3 on nucleus (all 3 used)	256 (up to 25 curves per cell used)	256 (up to 25 curves per cell used)	~5	~5
Indentation location on the cell	Above the nucleus and near the edge (for nucleus and cytoplasm)	Above the nucleus	Above the nucleus		Cytoplasm between the cell nucleus and it’s edge	
Variance in Young's modulus over the cell surface measured	Edge vs nucleus: ~40% in mean, ~15% in median	N/A	~35 %	~60 % at 300 nm indentation depth	6.9834 kPa	0.103 kPa
How the location was identified	Microscope observation (brightfield)		surface points around the top when the incline of the surface is <10-15 degrees (surface profile was found in Force-Volume mode)		Microscope observation (brightfield)	